Polarization of top produced in particle decays in an arbitrary frame

Arunprasath V.* and Rohini M. Godbole†
Centre for High Energy Physics, Indian Institute of Science, Bengaluru, 560012

Ritesh K. Singh‡
Department of Physical Sciences, Indian Institute of Science Education and Research Kolkata, Mohanpur, 741246, India

In most of the models beyond the Standard Model, the top quark is expected to be polarized when produced in the decay of some heavier particle, like the gluino or the stop. The polarization is constructed, in an experiment or in simulations, through the distribution of top decay products. Here, we propose an estimator of top quark polarization that depends only on the kinematics of it's mother particle, apart from its decay couplings to top quarks, and is given in terms of the top polarization expected in the rest frame of the decaying particle. This estimator allows one to estimate the top polarization without performing a full simulation. We find this estimator is independent of the production angle of the mother, top decay angle (for unpolarized mother), and the spin of the mother particle. We study the quality of the estimator with finite width of the mother particle via examples of gluinos and stops decaying into top quark at LHC. We also point out how for the mass spectra of gluinos and top squarks currently expected in a 'natural' scenario, the polarization of the top quarks produced in the gluino decays can uniquely track the mixing angle in the stop sector.

arXiv:1612.03803v1 [hep-ph] 12 Dec 2016

I. INTRODUCTION

The top quark is the heaviest known fundamental particle of the SM. The LHC produces top quarks copiously, enabling a precision study of it's properties [1–6]. The importance of the studies of the top quark's properties lies not only in the validation of the SM in the top sector but also in probing effects of any possible new physics (NP). Since the mass of the top quark is close to the EW symmetry breaking scale, it is expected to play an important role in the electroweak symmetry breaking [7, 8]. One of the important properties of the top quark is that it decays before hadronization sets in. This property makes it possible to obtain information on top spin through the kinematic distributions of the decay products [9–11].

The polarization of the produced top quark is determined by the production mechanism and hence varies from process to process. For example, the polarization of the top in the $t\bar{t}$ production process is negligible due to the parity conserving nature of the strong interaction – a purely vector interaction. The top polarization in $t\bar{t}$ production is about 0.4% for 14 TeV LHC, at NLO in QCD with 1-loop weak and QED corrections. This is the value in the so called helicity basis where the spin quantization axis is along the direction of motion of the top [12]. On the other hand, the weak interaction mediated top production process, the single top production, produces highly polarized top quarks due to the $V-A$ nature of the interaction. For example, in the spectator basis, where the top spin quantization direction is taken along the direction of the light quark jet that scatters away from the top quark, the single top production process produces a top polarization of about -0.99 [13, 14], at leading order. In the helicity basis, in the center of mass frame of the top quark and the spectator jet, the single top polarization is about 0.99, at leading order [13, 14]. Polarized top quarks can also be produced in processes of various Beyond the Standard Model (BSM) scenarios, such as, minimal supersymmetric standard model (MSSM) [15–19], R-parity violating MSSM [20, 21], warped extra dimensions [22, 23], little Higgs [24] etc. Any new physics affecting the top production and which is chiral in nature can affect the polarization of the top. Hence, top polarization can be used as a signature of new physics in the top production [17, 18, 23–37].

In many of the BSM scenarios mentioned above, the top quark can be produced through the decays of some heavy particle postulated therein [15, 17–19]. In these cases, the top polarization is determined in the rest frame of the mother particle by dynamical parameters of the interactions that are responsible for the decay of the mother particle and is given by a simple analytical expression. However, in the frame where the top polarization is measured, laboratory frame (say), the decaying mother particle is not at rest, in general[1]. Since the top helicity states are not invariant under arbitrary Lorentz transformations the top polarization measured in the laboratory (lab) frame is not the same as the one given in the rest frame of the mother particle. The two values are

* arunprasath@cts.iisc.ernet.in
† rohini@cts.iisc.ernet.in
‡ ritesh.singh@iiserkol.ac.in

[1] Measurement of top polarization in the laboratory frame has the advantage that it does not require the reconstruction of the rest frame of the top quark. An estimation of top polarization that would be observed in the laboratory frame is useful in the construction of appropriate top spin observables. Our work illustrates some of the important issues in the estimation of lab frame top polarization.

related by a kinematical factor which, in general, would depend on the direction and magnitude of the Lorentz boost required to reach the lab frame (or any frame where the mother particle is moving) from the rest frame of the mother particle. In this work we determine the kinematic factor and provide its explicit analytical expression, assuming that the mother particle is unpolarized and has a narrow width. We choose two processes where the top is produced through the decay of another particle: $pp \to \tilde{g}\tilde{g} \to \tilde{g}t\tilde{t}_1^*$, and $pp \to \tilde{t}_1^*\tilde{t}_1 \to \tilde{t}_1^* t\tilde{\chi}_1^0$. These processes can be written in a general form:

$$pp \to A + A \to A + (t + B) \tag{1}$$

where A is the heavy particle which decays[2] as $A \to t+B$. For these processes, we provide an estimator of top polarization $\mathcal{P}_{estimator}$ which can give an estimate of top polarization without simulating the heavy particle decay and using simply the kinematical distribution of the mother particle A. This estimator can be written as a convolution of the top polarization in the rest frame of the mother particle which is determined by the kinematic and dynamical factors mentioned above, and the velocity distribution of the mother particle in that frame. Since the velocity distribution of the mother particle is determined by the (parton distribution function) PDF factors of the *pp* collision, this estimate of the top polarization can be understood as a weighted average of top polarization over the entire sample of events.

$$\mathcal{P}_{estimator} \equiv \frac{1}{\sigma_{AA}} \int \frac{d\sigma_{AA}}{d\beta_A} \ \mathcal{P}(\beta_A). \tag{2}$$

Here, σ_{AA} is the cross section for the pair production of A in the process: $pp \to A\bar{A}$ and β_A is the velocity of A in the given frame. In the following discussions we choose this frame to be either the lab frame or the parton center of mass (PCM) frame. We find that $\mathcal{P}(\beta_A)$ in any chosen frame depends not on the direction of emission of the unpolarized mother particle A in that frame but only the magnitude of its velocity. We find that the estimator gives a good approximation of the true value of top polarization when the events are dominated by events where the mother particle is on-shell. When the sample of events is dominated by off-shell decays of the mother, a good estimation of top polarization can be obtained, in the case of scalar mother, by assuming that the mass of the mother is distributed as Breit-Wigner distribution. We find that this does not work very well for the case of spin-1/2 mother particle and we explain the reason behind it.

We choose these examples of gluino/stop pair production and their decay for their phenomenological importance, as explained in the following. After the LHC discovery of a light Higgs with SM-like couplings and a mass about 125 GeV [38, 39], questions on the naturalness in the Higgs sector of the SM have become urgent. Given the light Higgs mass of 125 GeV, models within the framework of MSSM, typically require, a large stop mixing, stop mass eigenstates with masses $\sim 1\ TeV$, and a heavy gluino [40–42]. However, Higgs sector can be also natural and be consistent with the observation of a light Higgs, in models where one of the two stop mass eigenstates is light ($0.5 - 1.0$ TeV) and the other one is heavy (~ 1.0 TeV) [43–45]. When one of the stop mass eigenstates is light and when gluinos are not too heavy so that their production cross section remains accessible at the LHC, the corresponding model parameters can be probed at the LHC through the polarization of top quarks produced in their decays. The top quark produced in the decay of a gluino or a stop is expected to be polarized because of the chiral nature of its coupling with the gluino or the stop, since the mass eigenstate $\tilde{t}_1$ (say) is an arbitrary mixture of $\tilde{t}_L$ and $\tilde{t}_R$ and the neutralino $\tilde{\chi}_1^0$ is an arbitrary mixture of higgsino and gaugino.

In the decays of a gluino where a top is produced, $\tilde{g} \to \tilde{t}_1^* t$ and $\tilde{g} \to \tilde{t}_2^* t$, the polarization of the top produced is a direct measure of the stop mixing angles, as we shall show in Section II. On the other hand, when the top is produced from the decay of a stop, the top polarization in the stop rest frame depends not only on the stop mixing angle but also on gaugino and higgsino content of the neutralino [15, 18, 46, 47]. Hence, it is interesting to calculate top polarization in gluino decays though the cross sections may be smaller as the limits on gluino masses have already touched $\sim$ TeV. The stop decays, on the other hand, can have higher cross sections as the LHC data allows them to be much lighter compared to a gluino, though the top polarization now depends additionally on parameters such as mixing in the neutralino sector. Hence, we consider in this work both the decays and calculate in each case the top polarization as a function of model parameters.

This paper is organized as follows. Section II discusses the evaluation of top polarization in the rest frames of a gluino and a stop respectively. Section III describes the formalism of our work and a derivation of our main result. Section IV describes the procedure to obtain the top polarization at the level of *pp* collisions. In Section V we describe the numerical work with which we validate our analytical result. We conclude in Section VI and present some of the calculational details in the appendix.

II. TOP POLARIZATION IN THE REST FRAME OF THE DECAYING PARTICLE

A. Gluino decay

The gluino decay mode of interest are the ones involving the top quark: $\tilde{g} \to t\tilde{t}_1^*$ and $\tilde{g} \to t\tilde{t}_2^*$. Here $\tilde{t}_1$ and $\tilde{t}_2$ are the lighter and the heavier of stop mass eigenstates,

[2] We mostly assume that the unstable particle A has a narrow width i.e., $\Gamma_A/M_A \ll 1$ and also that the masses of A, B, t are widely separated, but later generalize to the case where the narrow width approximation is lifted for the particle A.

respectively. The interaction of a top, a gluino and a stop mass eigenstate depends only on the stop mixing angle $\theta_{\tilde{t}}$, when mixing with first two generations is neglected. The stop mixing angle relates the two mass eigenstates of the stop ($\tilde{t}_1$, $\tilde{t}_2$) to their interaction eigenstates $\tilde{t}_L$ and $\tilde{t}_R$:

$$\begin{aligned}\tilde{t}_1 &= \cos\theta_{\tilde{t}}\tilde{t}_L + \sin\theta_{\tilde{t}}\tilde{t}_R, \\ \tilde{t}_2 &= -\sin\theta_{\tilde{t}}\tilde{t}_L + \cos\theta_{\tilde{t}}\tilde{t}_R.\end{aligned} \tag{3}$$

The interaction of the stop with the gluino and the top is given by the following Lagrangian, again in the approximation that there is no flavor-mixing between the first two generations and the third generation:

$$\mathcal{L}_{\tilde{t}\tilde{g}t} = -\sqrt{2}g_3\left\{\bar{t}[W_{3i}P_R - W_{6i}P_L]T^a\tilde{g}^a\tilde{t}_i\right\} + \text{h.c.} \tag{4}$$

In the above expression, g_3 denotes the strong coupling constant, $i = 3, 6$ the stop mass eigenstates $(\tilde{t}_1, \tilde{t}_2)$, $a = 1, \cdots 8$ the adjoint $SU(3)_c$ indices and P_L, P_R the chirality projecting operators. The color indices of the top and the stop mass eigenstates have been suppressed. The sfermion mixing matrix is denoted by W and it's elements are:

$$W_{33} = W_{66} = \cos\theta_{\tilde{t}}, \qquad W_{36} = -W_{63} = \sin\theta_{\tilde{t}} \tag{5}$$

where $\theta_{\tilde{t}}$ is the stop mixing angle. To derive the expression for top polarization in the gluino rest frame, one begins by writing down the amplitude for the process and evaluating the partial width Γ^λ of the gluino decaying into a stop and a top with a helicity λ. Then the top polarization in the gluino rest frame is given by the formula:

$$\mathcal{P}_0 = \frac{\Gamma^+ - \Gamma^-}{\Gamma^+ + \Gamma^-}. \tag{6}$$

The amplitudes for the gluino decay $\tilde{g} \to t\tilde{t}_1^*$ is as follows:

$$\begin{aligned}\mathcal{M}(\tilde{g} \to \tilde{t}_1 t) = &-\sqrt{2}\ g_3\ T^a \\ &\times \bar{u}(p_t, \lambda_t)(\cos\theta_{\tilde{t}}P_R - \sin\theta_{\tilde{t}}P_L)\ u(p_{\tilde{g}}, \lambda_{\tilde{g}})\end{aligned} \tag{7}$$

where λ_t and $\lambda_{\tilde{g}}$ denote the helicities of the top, and the gluino, respectively and t^a is the color factor. Squaring the amplitude and taking average over helicities and color indices of initial state particles and summing over the color indices of the top and the stop, we get

$$\begin{aligned}\Gamma^\lambda \propto \frac{g_3^2}{6}\Big[&(m_{\tilde{g}}^2 - m_{\tilde{t}}^2 + m_t^2 - 2m_{\tilde{g}}m_t\sin 2\theta_{\tilde{t}}) \\ &-2\lambda\cos 2\theta_{\tilde{t}}\ K^{1/2}(m_{\tilde{g}}^2, m_{\tilde{t}}^2, m_t^2)\Big].\end{aligned} \tag{8}$$

In the above expression, $K(x, y, z) = x^2 + y^2 + z^2 - 2xy - 2yz - 2zx$. Introducing the notation $\xi_t = m_t^2/m_{\tilde{g}}^2$ and $\xi_{\tilde{t}_1} = m_{\tilde{t}_1}^2/m_{\tilde{g}}^2$, we get

$$\mathcal{P}_0 = \frac{-K^{1/2}(1, \xi_t, \xi_{\tilde{t}_1})\cos 2\theta_{\tilde{t}}}{1 - \xi_{\tilde{t}_1} + \xi_t - 2\sqrt{\xi_t}\sin 2\theta_{\tilde{t}}}. \tag{9}$$

This choice of using top helicity states for spin states corresponds to the so-called helicity basis for the top polarization. We use this basis throughout this work.

B. Stop decay

The stop can decay in a number of modes, e.g., $\tilde{t}_1 \to \tilde{\chi}_i^0 t$, and $\tilde{t}_1 \to \tilde{\chi}_i^+ b$ etc. We consider the decays where a top quark is produced: $\tilde{t}_1 \to t\tilde{\chi}_i^0$ and $\tilde{t}_2 \to t\tilde{\chi}_i^0$ ($i = 1, \cdots, 4$). The vertex corresponding to the decay of a stop mass eigenstate, $\tilde{t}_{1,2} \to t\tilde{\chi}_1^0$, is given by the following Lagrangian,

$$\mathcal{L}_{\tilde{t}\tilde{\chi}^0 t} = \overline{\tilde{\chi}_1^0}\left[G^L P_L + G^R P_R\right]\tilde{t}_1^\dagger t + \text{h.c.} \tag{10}$$

The G^L and G^R in the above equation are as follows:

$$\begin{aligned}G^L &= -\frac{g_2}{\sqrt{2}}(N_{12} + \frac{1}{3}\tan\theta_W N_{11})\cos\theta_{\tilde{t}} - Y_t N_{14}\sin\theta_{\tilde{t}} \\ G^R &= -Y_t N_{14}^*\cos\theta_{\tilde{t}} + g_2\left(\frac{2\sqrt{2}}{3}\tan\theta_W N_{11}\sin\theta_{\tilde{t}}\right)\end{aligned} \tag{11}$$

where g_2 and Y_t are the $SU(2)_L$ and top Yukawa couplings, respectively and θ_W is the Weak mixing angle. N_{ij}, $(i, j = 1, \cdots, 4)$ in the above equation are the elements of the 4×4 neutralino mixing matrix. Note that the top quark is in the final state. This means that G^L and G^R correspond to the couplings of left and right chiral top quarks, respectively. The neutralino mixing matrix is the diagonalizing matrix of the mass matrix of the neutral gauginos (the bino, the wino) and the neutral higgsinos.

The expression for polarization of top quark produced in the process $\tilde{t}_1 \to t\tilde{\chi}_1^0$, evaluated in the stop rest frame is given in [15, 18, 19, 46, 47]. We sketch the derivation of expression for top polarization in the stop rest frame for sake of completeness. The amplitude for the stop decay $\tilde{t}_1 \to t\tilde{\chi}_1^0$ is given by:

$$\mathcal{M}(\tilde{t}_1 \to t\tilde{\chi}_1^0) = \bar{u}(p_t, \lambda_t)\left[G^L P_R + G^R P_L\right]v(p_{\tilde{\chi}}, \lambda_{\tilde{\chi}}). \tag{12}$$

Computing $\Gamma^\pm$, the partial width of the stop decaying into a neutralino and a top with a helicity $\lambda = \pm$ and using the expression Eq. (6), we get the required expression for the top polarization in stop rest frame as:

$$\mathcal{P}_0 = \frac{(|G^R|^2 - |G^L|^2)\ K^{1/2}(1, \eta_t, \eta_{\tilde{\chi}})}{(|G^R|^2 + |G^L|^2)(1 - \eta_t - \eta_{\tilde{\chi}}) - 4\sqrt{\eta_t\eta_{\tilde{\chi}}}\,\text{Re}(G^L G^{R*})} \tag{13}$$

where $\eta_t = m_t^2/m_{\tilde{t}_1}^2$ and $\eta_{\tilde{\chi}} = m_{\tilde{\chi}_1^0}^2/m_{\tilde{t}_1}^2$.

C. Polarization and mixing angles

Discussions of using polarization of the top quark produced in stop/sbottom decays $\tilde{t}_1 \to t\tilde{\chi}_1^0$ and $\tilde{b}_i \to t\tilde{\chi}_j^-$ $(i, j = 1, 2)$ to probe the mixing angle in the stop/sbottom sector exist in literature (see, for example, Refs. [15, 17, 48, 49]). But, as one can easily see from Eq. (9), top polarization in the gluino decays can probe the mixing angle in the stop sector irrespective of the mixing in the neutralino sector, given a value of

parameter	BP1	BP2	BP3
$m_{\tilde{g}}$	2290	2291	608
$m_{\tilde{\chi}_1^0}$	248	248	97
$m_{\tilde{t}_1}$	498	493	400
$\Gamma_{\tilde{g}}$	235	203	5.5
$\Gamma_{\tilde{t}_1}$	2.4	6.0	2.0
$\sin\theta_{\tilde{t}}$	0.0644	0.9979	0.8327
$\cos\theta_{\tilde{t}}$	0.9979	0.0642	0.5536
N_{11}	0.0953	-0.0988	0.9863
N_{12}	-0.0637	0.0619	-0.0531
N_{14}	-0.6939	0.6937	-0.0531
y_t	0.8507	0.8508	0.8928

TABLE I. The benchmark points used in this work. Masses and widths of the particles are given in GeV.

$\Delta m_{\tilde{g}} = m_{\tilde{g}} - m_{\tilde{t}_1}$. This is possible only when there is a large mass difference between $\tilde{t}_1$ and $\tilde{t}_2$. This can be seen as follows. Equation (9) gives the expression for the top polarization that is produced along with $\tilde{t}_1$ in the gluino decay. The corresponding expression for top polarization in the case of $\tilde{g} \to \tilde{t}_2 t$ can be obtained by the following interchange: $\sin\theta_{\tilde{t}} \to \cos\theta_{\tilde{t}}$, $\cos\theta_{\tilde{t}} \to -\sin\theta_{\tilde{t}}$ and $m_{\tilde{t}_1} \to m_{\tilde{t}_2}$. This means that $\cos 2\theta_{\tilde{t}} \to -\cos 2\theta_{\tilde{t}}$ and $\sin 2\theta_{\tilde{t}} \to -\sin 2\theta_{\tilde{t}}$ which changes the sign of the top polarization. If we count the tops from both $\tilde{g} \to \tilde{t}_1 t$ and $\tilde{g} \to \tilde{t}_2 t$ and if both stops are degenerate we get unpolarized tops. But, if there is a large mass difference between the two stops the net top polarization can be nonzero. When models in MSSM with a natural Higgs sector are realized in nature, we expect a large mass difference between the two stop mass eigenstates, as mentioned before. If we assume that the heavy stop $\tilde{t}_2$ is heavier than the gluino the tops can be polarized and this is the scenario which we focus on in this paper. In the case of stop decay, we consider decays of only light stop mass eigenstate $\tilde{t}_1$ since it can be accessible at colliders and partly because we focus on scenarios where the Higgs sector is natural. Hence, we study polarization of the top produced in the decay of a gluino into a top and $\tilde{t}_1$, for a few benchmark points. We also assume that the neutralino produced in the stop decay is the lightest of the four neutralino states.

The bench mark points used for numerical simulations are listed in Table I and corresponding top polarizations are listed in Tables II and III for reference. Here we have listed the rest frame polarization $\mathcal{P}_0$ along with the lab frame value $\mathcal{P}_{MC}$ obtained using full Monte-Carlo simulations. The lab frame values are usually reduced in magnitude due to change of quantization basis, as will be discussed in the next section. The proposed polarization estimators with narrow-width-approximation ($\mathcal{P}_{NW}$) and with Breit-Wigner folding ($\mathcal{P}_{BW}$), which can be directly compared to $\mathcal{P}_{MC}$, are also listed in Tables II and III for comparisons and will be discussed in latter sections.

Benchmark →	BP1	BP2	BP3
$\mathcal{P}_0$	−1.00	+1.00	+0.98
$\mathcal{P}_{MC}$	−0.99	+0.99	+0.51
$\mathcal{P}_{NW}$	−1.00	+1.00	+0.50
$\mathcal{P}_{BW}$	−0.98	+0.98	+0.51

TABLE II. List of top polarization in gluino decay at $\sqrt{s} = 13$ TeV LHC calculated for three benchmark in gluino rest frame $\mathcal{P}_0$, in the lab frame $\mathcal{P}_{MC}$ and using estimators $\mathcal{P}_{NW}$ and $\mathcal{P}_{BW}$ (see sections VI and V). The benchmark points BP1, BP2, and BP3 are given in Table I.

Benchmark →	BP1	BP2	BP3
$\mathcal{P}_0$	+0.92	−0.93	+0.97
$\mathcal{P}_{MC}$	+0.61	−0.60	+0.65
$\mathcal{P}_{NW}$	+0.61	−0.60	+0.65
$\mathcal{P}_{BW}$	+0.61	−0.60	+0.65

TABLE III. List of top polarization in stop decay at $\sqrt{s} = 13$ TeV LHC. Rest of the details are same as in Table II.

III. GENERAL FORMALISM

The cross section for the process in Eq. (1) can be written as

$$\sigma = \sum_{q_1,q_2} \int dx_1 dx_2 \; f_{q_1/p}(x_1) f_{q_2/p}(x_2) \times \; \hat{\sigma}(q_1 q_2 \to AA \to A + t + B) \qquad (14)$$

where the sum extends over all the parton flavors, q_1 and q_2. Since the top quark also decays, we can access its polarization through angular distribution of its decay products in the rest frame of the top quark. In the semi-leptonic decay of the top quark, the direction of motion of the charged lepton is 100% correlated with the top polarization, at leading order. In the top rest frame, we have:

$$\frac{1}{\Gamma}\frac{d\Gamma}{d\cos\theta_\ell} = \frac{1}{2}(1 + \mathcal{P}_0 \; \alpha_\ell \; \cos\theta_\ell). \qquad (15)$$

The coefficient α in the above equation is called the spin analyzing power and it is maximal for the charged lepton ($\alpha_\ell = 1$ at the LO of the SM). The value of $\mathcal{P}_0$ depends on the choice of quantization axis of the top quark. When the top spin quantization axis taken as its direction of motion in the rest frame of the gluino or the stop, the value of $\mathcal{P}_0$ is given by Eqs. (9) and (13) respectively.

The full amplitude of the process under consideration

is given by the following expression:

$$\mathcal{M} \sim \mathcal{M}'(p_1 p_2 \to AA)_\alpha \left(\frac{\not{p}_A + m_A}{(p_A^2 - m_A^2) + i m_A \Gamma_A}\right)_{\alpha'\alpha} \times \mathcal{M}'(A \to tB)_{\beta\alpha'} \left(\frac{\not{p}_t + m_t}{(p_t^2 - m_t^2) + i m_t \Gamma_t}\right)_{\beta'\beta} \times \mathcal{M}'(t \to b\bar{\ell}\nu)_{\beta'} \quad (16)$$

where the prime indicates that the amplitudes do not have their external fermion wave functions which are part of the propagators, the Greek indices denote the components of Dirac matrices and repeated indices are summed over. Squaring the amplitude and summing/averaging over the spins and color indices of the external states (which are suppressed in these expressions) gives the propagator factors of the form

$$\frac{1}{(p_A^2 - m_A^2)^2 + m_A^2 \Gamma_A^2}. \quad (17)$$

When the width of a particle is much smaller than its mass, the narrow width approximation (NWA) can be used which consists of the following replacement for the propagators:

$$\frac{1}{(p^2 - m_A^2)^2 + \Gamma_A^2 m_A^2} \to \frac{\pi}{m_A \Gamma_a} \delta(p^2 - m_A^2)\theta(p^0) \quad (18)$$

Similar replacements can be made for all the other intermediate particles, including the top quark. Under this approximation, the production of a particle and its decay are separated as factors with spin-correlations. This is made possible, in the narrow width approximation, because of the following relation for the numerator of a propagator (for a spin-1/2 particle)

$$\not{p} + m = \sum_\lambda u(p,\lambda)\bar{u}(p,\lambda) \quad (19)$$

where λ denotes the helicity state of the particle, defined with respect to the momentum p (its spin quantization axis). Using this relation in the numerator of Eq. (16), we get,

$$\mathcal{M}^{\rm num} \sim \sum_{\lambda_A,\lambda_t} \bar{u}(p_A,\lambda_A)\mathcal{M}'^{\rm num}(p_1 p_2 \to AA) \times \bar{u}(p_t,\lambda_t)\mathcal{M}'^{\rm num}(A \to tB)u(p_A,\lambda_A) \times \mathcal{M}'^{\rm num}(t \to b\bar{\ell}\nu)u(p_t,\lambda_t) \quad (20)$$

$$= \sum_{\lambda_A,\lambda_t} \mathcal{M}^{\rm num}(p_1 p_2 \to AA)_{\lambda_A} \mathcal{M}^{\rm num}(A \to tB)_{\lambda_A,\lambda_t} \times \mathcal{M}^{\rm num}(t \to b\bar{\ell}\nu)_{\lambda_t} \quad (21)$$

Squaring the amplitude $\mathcal{M}$ and performing the replacements of Eq. (18), in the case of gluino ($A = \tilde{g}$), we get

$$\hat{\sigma}(\hat{s}) = \int d\Omega \sum_{\{\lambda\}} \left(\frac{d\hat{\sigma}_{\tilde{g}\tilde{g}}}{d\Omega}\right)_{\lambda_{\tilde{g}}\lambda'_{\tilde{g}}} \left(\frac{d\Gamma_{\tilde{g}}}{\Gamma_{\tilde{g}}}\right)^{\lambda_{\tilde{g}}\lambda'_{\tilde{g}}}_{\lambda_t\lambda'_t} \left(\frac{d\Gamma_t}{\Gamma_t}\right)_{\lambda_t\lambda'_t} \quad (22)$$

at the parton level. Similar parton level calculations in the case of stop yields a simpler expression, given as:

$$\hat{\sigma}(\hat{s}) = \int d\Omega \sum_{\{\lambda\}} \frac{d\hat{\sigma}_{\tilde{t}\bar{t}}}{d\Omega} \left(\frac{d\Gamma_{\tilde{t}}}{\Gamma_{\tilde{t}}}\right)_{\lambda_t\lambda'_t} \left(\frac{d\Gamma_t}{\Gamma_t}\right)_{\lambda_t\lambda'_t}. \quad (23)$$

In these expressions, the parton level differential cross section (density matrix) for the pair production of gluinos is denoted by $(d\hat{\sigma}_{\tilde{g}\tilde{g}}/d\Omega)_{\lambda_{\tilde{g}}\lambda'_{\tilde{g}}}$. The spin indices (helicities, in our case) of all other intermediate particles are summed over.

When the gluino is unpolarized, as it would be in the case of QCD production, the production cross section (density matrix) for gluino pairs (see Eq. (22)) can be written as $(d\hat{\sigma}_{\tilde{g}\tilde{g}}/d\Omega)_{\lambda_{\tilde{g}},\lambda'_{\tilde{g}}} = (d\hat{\sigma}_{\tilde{g}\tilde{g}}/d\Omega)\ (\delta^{\lambda_{\tilde{g}}\lambda'_{\tilde{g}}}/2)$ where $\lambda_{\tilde{g}},\ \lambda'_{\tilde{g}}$ are the helicity states of the intermediate gluino. On summing over gluino helicities, the differential cross-section of gluino pair production becomes a multiplicative factor in just the same way as $d\hat{\sigma}_{\tilde{t}\bar{t}}/d\Omega$ does in the case of stop decay (Eq. (23)). We emphasize here that the helicities are defined in the frame in which the top polarization needs to be defined. We first take the frame in which Eq. (22) and Eq. (23) are defined to be the corresponding parton center of mass (PCM) frame. This frame can be reached from the top rest frame in two ways: (i) a direct Lorentz boost along the direction of top in the PCM frame, (ii) a Lorentz boost to the rest frame of the mother particle along the direction of top momentum in that frame followed by a Lorentz transformation to the PCM frame which is, in general, not in the direction of top momentum. As result, the helicity states of the top in the two cases are not identical. This affects the value of top polarization measured in the PCM frame. It turns out that the helicity states of the top in the latter case can be written as a rotation of the helicity states defined in the PCM frame. Note that this procedure is also applicable to the calculation of top polarization in the lab frame. However, the top polarization in lab frame can be obtained without going through the parton center of mass frame, as will be discussed in Section IV.

A. Helicity and Lorentz boosts

As mentioned before, the helicity of a particle is not invariant under Lorentz boosts in general. The helicity state $|p,\lambda\rangle$ transforms under a Lorentz boost as

$$|p,\lambda\rangle = R_{\lambda\lambda'}|p',\lambda'\rangle \quad (24)$$

where $|p',\lambda'\rangle$ is the helicity state of the particle after the Lorentz boost has been applied [50]. The helicity states $|p,\lambda\rangle$ are constructed from the eigen states of spin in the rest frame of the particle by a series of transformations: $|p,\lambda\rangle = R_z(\phi)R_y(\theta)\Lambda_z(\beta)|m,s_z = \lambda\rangle$, where θ,ϕ and β are the angles and the velocity of the particle. With this convention for helicity states, the coefficients $R_{\lambda,\lambda'}$ in

Eq. (24) can be given in the following form of a rotation matrix

$$R = R_z(-\chi)R_y(-\omega) \tag{25}$$

where, χ and ω are some angles which depend on the direction and magnitude of the Lorentz boost applied on $|p,\lambda\rangle$. Expressions for χ and ω are given in Appendix A.

B. Gluino decay

In the rest frame of the gluino[3] which decays into a top, the differential decay width which appears in Eq. (22) is given by

$$\int\left(\frac{\mathrm{d}\Gamma_{\tilde{g}}}{\Gamma_{\tilde{g}}}\right)_{\lambda\lambda'} = \frac{m_g}{64\pi^2\Gamma_{\tilde{g}}}\,\frac{4\pi\alpha_S}{9}\int \mathrm{d}\cos\theta_t^{\tilde{g}}\;\mathrm{d}\phi_t^{\tilde{g}} \times\Big[\delta_{\lambda\lambda'}\left(\frac{1}{2}(1-\xi_{\tilde{t}}+\xi_t)-\sqrt{\xi_t}\sin 2\theta_{\tilde{t}}\right) -\cos 2\theta_{\tilde{t}}\sqrt{\xi_t}\beta\gamma\sigma^3_{\lambda\lambda'}\Big]. \tag{26}$$

$\xi_t, \xi_{\tilde{t}_1}$ have been defined in Section II. The velocity of the top in the above equation is given by $\beta = K^{1/2}(1,\xi_t,\xi_{\tilde{t}_1})/(1-\xi_{\tilde{t}_1}+\xi_t)$ and $\gamma = 1/\sqrt{1-\beta^2}$. The helicity states of the top quark λ,λ' in the above equation are defined with respect to the top momentum in the gluino rest frame. For top decaying in the semi-leptonic channel $t\to b\bar{\ell}\nu$ (with narrow width approximation for the top as well as the W boson) the differential decay width is given by

$$\int\frac{\mathrm{d}\Gamma_t}{\Gamma_t} = \int \mathrm{d}x_\ell \mathrm{d}\Omega_\ell\;\frac{G_F^2 m_t^5\;x_\ell(1-x_\ell)}{64\pi^3\bar{\Gamma}_W r_t\Gamma_t}\;(\delta_{\lambda\lambda'}+\hat{p}_\ell\cdot\vec{\sigma}_{\lambda\lambda'}) \tag{27}$$

where $r_t = m_t^2/m_W^2$, $\bar{\Gamma}_W = \Gamma_W/m_W$, $x_\ell = 2E_\ell/m_t$ with $1/r_t \le x_\ell \le 1$. The direction of the momentum of the charged lepton from decay of the top, in the top rest frame, is denoted in the above equation as $\hat{p}_\ell$. Hence,

$$\frac{d\Gamma_{\tilde{g}}}{\Gamma_{\tilde{g}}}^{\mathrm{PCM}} = R\left(\frac{d\Gamma_{\tilde{g}}}{\Gamma_{\tilde{g}}}\right)R^\dagger, \tag{28}$$

and

$$\frac{d\Gamma_t}{\Gamma_t}^{\mathrm{PCM}} = \frac{d\Gamma_t}{\Gamma_t}. \tag{29}$$

The rotation matrix R in Eq. (28) is given in Eq. (25). Substituting the expressions for the differential decay widths for $\tilde{g}\to t\tilde{t}_1^*$ and $t\to b\bar{\ell}\nu$ from Eqs. (26), (27), we get

$$\frac{\mathrm{d}\hat{\sigma}}{\mathrm{d}x_\ell \mathrm{d}\cos\theta_{t\ell}\mathrm{d}\phi_{t\ell}} \propto \int\frac{\mathrm{d}\hat{\sigma}_{\tilde{g}\tilde{g}}}{\mathrm{d}\Omega_{\tilde{g}}}\;\Big[1+\mathcal{P}_0\;\cos\omega\cos\theta_{t\ell} - \mathcal{P}_0\;\sin\omega\sin\theta_{t\ell}\cos(\phi_{t\ell}+\chi)\Big] \times x_\ell(1-x_\ell)\;\mathrm{d}\Omega_g\;\mathrm{d}\Omega_t^{\tilde{g}}. \tag{30}$$

where $\hat{\sigma}$ is the cross section for the full parton level process $q_1q_2\to\tilde{g}\tilde{g}\to\tilde{g}\tilde{t}_1^* b\bar{\ell}\nu$, $\mathcal{P}_0$ is the value of top polarization in the rest frame of the gluino.

Let $I(\bar{\beta}(\hat{s})) = \frac{1}{2}\int\cos\omega\;\mathrm{d}\cos\theta_t^{\tilde{g}}$. Integrating Eq. (30) over all variables except $\theta_{t\ell}$, we get

$$\frac{\mathrm{d}\hat{\sigma}}{\mathrm{d}\cos\theta_{t\ell}} = \hat{\sigma}_{\tilde{g}\tilde{g}}(\hat{s})\;\mathcal{B}(\tilde{g}\to t\tilde{t}_1^*)\;\mathcal{B}(t\to b\bar{\ell}\nu) \times\frac{1}{2}(1+\mathcal{P}_0 I(\bar{\beta})\;\cos\theta_{t\ell}) \tag{31}$$

where $\hat{\sigma}_{\tilde{g}\tilde{g}}(\hat{s})$ denotes the parton level cross-section for pair production of gluinos. Note that the angle χ drops out of Eq. (31). The coefficient of $\cos\theta_{t\ell}$ can be interpreted as the polarization of the top as given by the lepton angular distribution in the top rest frame. The helicity rotation angle ω is independent of the direction of motion of the gluino in the parton center of mass frame (see Appendix A), so is the polarization of the top. The expressions for $I(\bar{\beta})$ are as follows:

$$\begin{aligned} I(\bar{\beta}) &= \frac{1}{2\beta^2\bar{\beta}}\left[2\bar{\beta}-(1-\beta^2)\log\left(\frac{1+\bar{\beta}}{1-\bar{\beta}}\right)\right]\quad(\beta>\bar{\beta})\\ &= \frac{1}{2\beta^2\bar{\beta}}\left[2\beta-(1-\beta^2)\log\left(\frac{1+\beta}{1-\beta}\right)\right]\quad(\beta<\bar{\beta}) \end{aligned} \tag{32}$$

Substituting the value of top velocity β in the gluino rest frame, we get the following expression which is valid for both cases, viz., $\beta>\bar{\beta}$ and $\beta<\bar{\beta}$:

$$\begin{aligned} \mathcal{P}(\bar{\beta}) &= I(\bar{\beta})\mathcal{P}_0\\ &= \frac{\mathcal{P}_0}{2\bar{\beta}K}\times\Big[(1-\xi_{\tilde{t}_1}+\xi_t)\Big((K^{1/2}+\bar{\beta}(1-\xi_{\tilde{t}_1}+\xi_t))\\ &\quad -|K^{1/2}-\bar{\beta}(1-\xi_{\tilde{t}_1}+\xi_t)|\Big)\\ &\quad -4\xi_t\log\left(\frac{\Delta_1+K^{1/2}+\bar{\beta}(1-\xi_{\tilde{t}_1}+\xi_t)}{\Delta_2+|K^{1/2}-\bar{\beta}(1-\xi_{\tilde{t}_1}+\xi_t)|}\right)\Big] \end{aligned} \tag{33}$$

where, $K\equiv K(1,\xi_{\tilde{t}_1},\xi_t)$ and $\Delta_{1,2} = (1-\xi_{\tilde{t}_1}+\xi_t)(1\pm\beta\bar{\beta}) = (1-\xi_{\tilde{t}_1}+\xi_t)\pm\bar{\beta}K^{1/2}(1,\xi_{\tilde{t}_1},\xi_t)$. This expression can also be written as

$$\begin{aligned} \mathcal{P}(\bar{\beta}) &= \frac{\mathcal{P}_0}{2\bar{\beta}K}\Bigg[(1-\xi_{\tilde{t}_1}+\xi_t)\\ &\quad\times\Big(\sqrt{\Delta_1^2-4(1-\bar{\beta}^2)\xi_t}-\sqrt{\Delta_2^2-4(1-\bar{\beta}^2)\xi_t}\Big)\\ &\quad -4\xi_t\log\left(\frac{\Delta_1+\sqrt{\Delta_1^2-4(1-\bar{\beta}^2)\xi_t}}{\Delta_2+\sqrt{\Delta_2^2-4(1-\bar{\beta}^2)\xi_t}}\right)\Bigg]. \end{aligned} \tag{34}$$

[3] We have taken z-axis of the lab frame coordinate system along one of the beam directions and the x-axis in a plane containing the top momentum and the beam axis and the y- axis along the normal to this plane. The azimuthal angle of the top, in the parton center of mass frame and in the lab frame $\phi = 0$, due to this choice of the coordinate system. All the angles that have been mentioned so far correspond to this coordinate system.

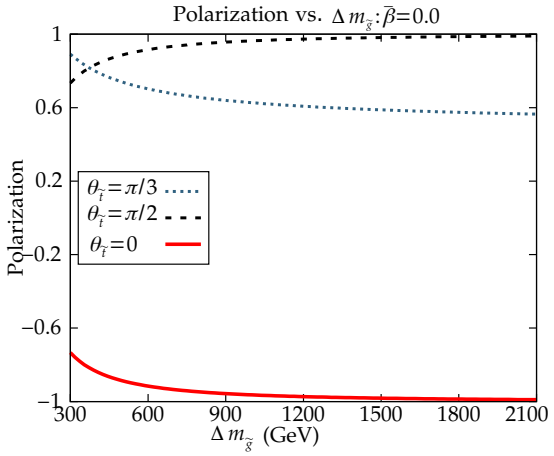

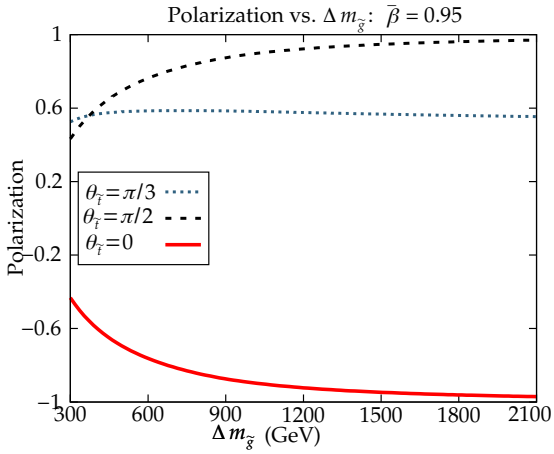

FIG. 1. The top polarization as a function of $\Delta m_{\tilde{g}} = m_{\tilde{g}} - m_{\tilde{t}_1}$, for two different values of the velocity of gluino: $\bar{\beta} = 0.0$ (top) and $\bar{\beta} = 0.95$ (bottom).

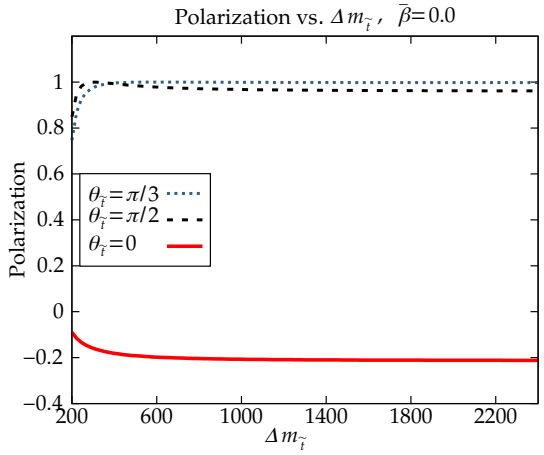

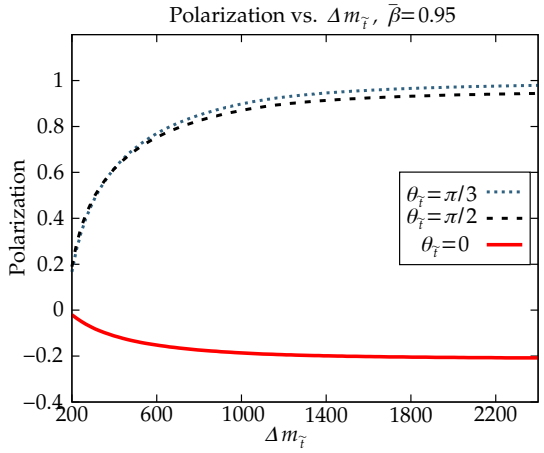

FIG. 2. Top polarization as a function of $\Delta m_{\tilde{t}} = m_{\tilde{t}_1} - m_{\tilde{\chi}_1^0}$ for different values of the velocity of the stop ($\bar{\beta}$): $\bar{\beta} = 0.0$ (top) and $\bar{\beta} = 0.95$ (bottom). The neutralino are bino-like. $N_{11} \approx 1$, $N_{12}, N_{14} \approx 0$, where $N_{ij} (i, j = 1, \cdots, 4)$ denote the neutralino mixing matrix elements.

C. Stop decay

Analogous to Eq. (34), the expression for polarization of the top, in the PCM frame where the mother stop is moving with a velocity $\bar{\beta}$ is the following:

$$\mathcal{P}(\bar{\beta}) = \frac{\mathcal{P}_0}{2\bar{\beta}K}\Bigg[(1+\eta_t-\eta_{\tilde{\chi}}) \times\left(\sqrt{\Delta_1^2-4(1-\bar{\beta}^2)\eta_t}-\sqrt{\Delta_2^2-4(1-\bar{\beta}^2)\eta_t}\right) - 4\eta_t\log\left(\frac{\Delta_1+\sqrt{\Delta_1^2-4(1-\bar{\beta}^2)\eta_t}}{\Delta_2+\sqrt{\Delta_2^2-4(1-\bar{\beta}^2)\eta_t}}\right)\Bigg] \quad (35)$$

where $\Delta_{1,2} = 1+\eta_t-\eta_{\tilde{\chi}} \pm \bar{\beta}K^{1/2}(1, \eta_t, \eta_{\tilde{\chi}})$. Eqs. (9) and (13) show that $\mathcal{P}_0$ is a function of $\Delta m_{\tilde{g}/\tilde{t}_1}$ and the mixing angle $\theta_{\tilde{t}}$. Thus, $\mathcal{P}$ depends not only on $\bar{\beta}$ but also on the mass difference and the mixing angle. Figs. 1 and 2 show $\mathcal{P}$ as a function of $\Delta m_{\tilde{g}/\tilde{t}}$ for different choices of $\theta_{\tilde{t}}$ and $\bar{\beta}$. In the stop case, the neutralino is assumed to be bino-like with $N_{11} \approx 1$, $N_{12}, N_{14} \approx 0$. The function $I(\bar{\beta})$ for small values of $\Delta m_{\tilde{g}/\tilde{t}}$, i.e. for small values of β (velocity of the top in the rest frame of the mother particle) varies as $\beta/\bar{\beta}$ according to Eq. (32). For large values of $\Delta m_{\tilde{g}/\tilde{t}}$ such that $\beta > \bar{\beta}$, $I(\bar{\beta})$ goes as $1/\beta^2$ which remains close to unity. Hence, $I(\bar{\beta})$ in these cases changes rapidly as a function of $\Delta m_{\tilde{g}/\tilde{t}}$ and approaches its limiting value asymptotically as $\Delta m_{\tilde{g}/\tilde{t}}$ increases further towards large values. This explains the rapid rise of the magnitude of top polarization with increasing Δm for $\theta_{\tilde{t}} = \pi/2$ and $\theta_{\tilde{t}} = 0$, in the case of gluino decay. The case of stop decay is also qualitatively similar, as seen from Fig. 2.

Fig. 3 (Fig. 4) show the top polarization as a function of the velocity of the gluino (stop) $\bar{\beta}$ for different choices of $\theta_{\tilde{t}}$ and $\Delta m_{\tilde{g}} = m_{\tilde{g}} - m_{\tilde{t}_1}$ ($\Delta m_{\tilde{t}} = m_{\tilde{t}_1} - m_{\tilde{\chi}_1}$). From Eq. (32) we can see that the function $I(\bar{\beta})$ remains independent of $\bar{\beta}$ for small values of $\bar{\beta}$ ($I(\bar{\beta}) \propto 1/\beta^2[1-(1-\beta^2)(1+\mathcal{O}(\bar{\beta}^2))]$) and falls as $1/\bar{\beta}$ for large values of $\bar{\beta}$ ($> \beta$). This can be seen clearly from Fig. 3 and Fig. 4. These figures also show that the value of

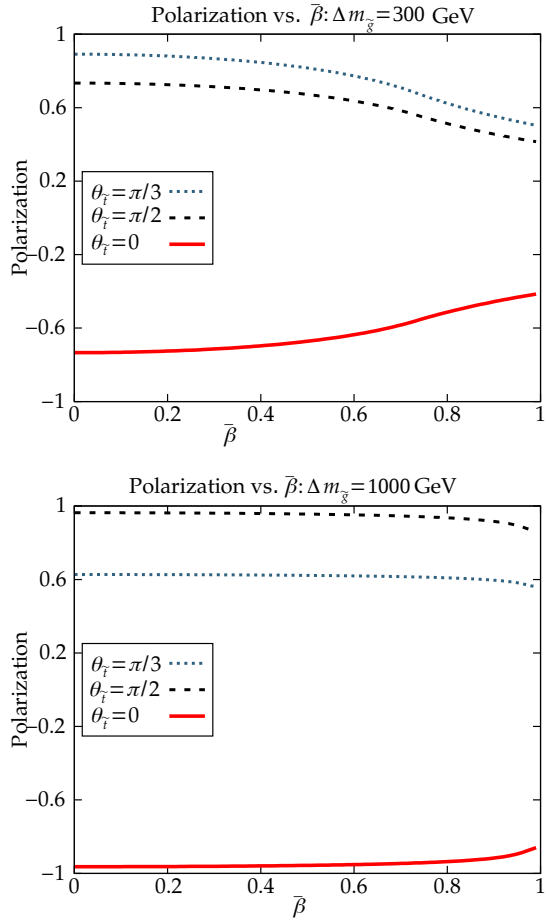

FIG. 3. The top polarization as a function of velocity $\bar{\beta}$ of the gluino, for two different values of $\Delta m_{\tilde{g}} = m_{\tilde{g}} - m_{\tilde{t}_1}$: $\Delta m_{\tilde{g}} =$ 300 GeV (top) and $\Delta m_{\tilde{g}} = 1000$ GeV (bottom).

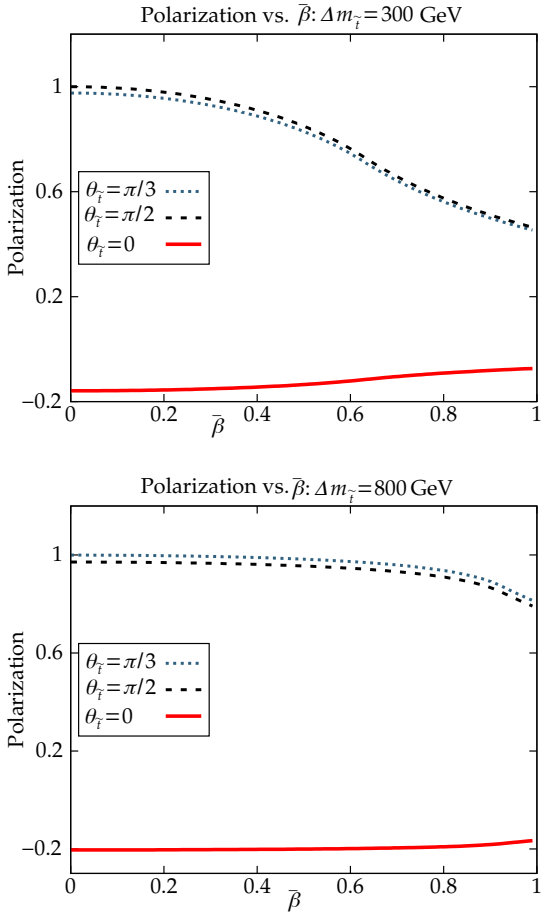

FIG. 4. Top polarization as a function of the boost $\bar{\beta}$ of the stop, for two different values of the mass difference between the stop and the neutralino ($\Delta m_{\tilde{t}} = m_{\tilde{t}_1} - m_{\tilde{\chi}_1^0}$): $\Delta m_{\tilde{t}} = 300$ GeV (top) and $\Delta m_{\tilde{t}} = 800$ GeV (bottom). The rest of the parameters are the same as those in Fig. 2.

$\Delta m_{\tilde{g}/\tilde{t}}$ determines the value of $\bar{\beta}$ at which the function $I(\bar{\beta})$ and hence the top polarization $\mathcal{P}(\bar{\beta})$ starts to fall as $1/\bar{\beta}$.

Some of the previous works [17–19] have pointed out the need to consider the effects of kinematics on the top polarization when it is measured in the lab frame,in cases where the top is produced in the decays of heavy SUSY particles. But our work is new in the sense that we have given explicit expressions for the top polarization in the case of gluino decay which has not been considered in the literature so far. Although Ref. [19] has outlined the method of obtaining the top polarization when the top is produced in the decays of other particles, we feel that a detailed deviation of the expression for top polarization would serve to clarify the issues such as the absence of dependence of top polarization on the direction of motion of the decaying particle.

IV. TOP POLARIZATION IN pp COLLISIONS

Note that Eqs. (34) and (35) are at parton level. The polarization of the top at the level of pp collisions can be obtained by convoluting Eq. (34) and Eq. (35) with the parton distribution functions of the proton. In the case of gluino decay, this gives the top polarization $\mathcal{P}_{NW}$ in the pp collision as a weighted average over the parton center of mass frame velocities of the gluino (similar expressions hold for the case of stop decay):

$$\mathcal{P}_{NW} = \frac{1}{\sigma_{\tilde{g}\tilde{g}}} \sum_{q_1,q_2} \int dx_1 dx_2 \; f_{q_1/p}(x_1) f_{q_2/p}(x_2) \; \hat{\sigma}_{\tilde{g}\tilde{g}}(\hat{s}) \mathcal{P}(\bar{\beta}) \tag{36}$$

where $\sigma_{\tilde{g}\tilde{g}}$ is the cross section for the production of a gluino pair. The total cross section of the full process

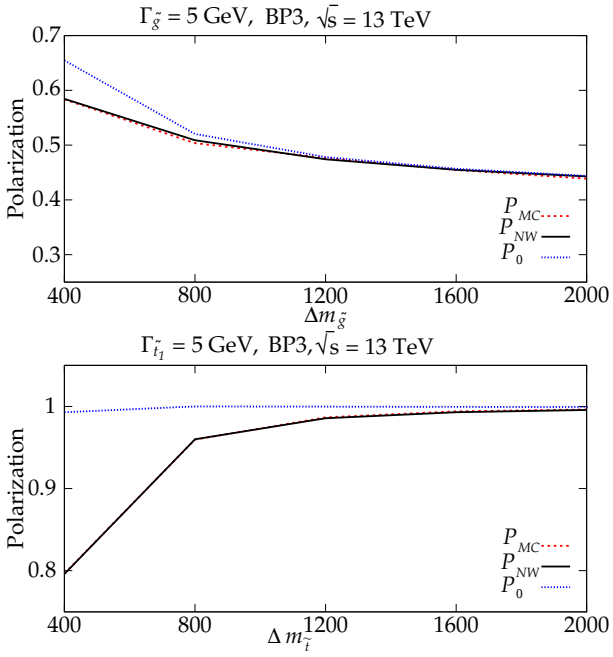

FIG. 5. Comparison of $\mathcal{P}_0$, $\mathcal{P}_{MC}$ and $\mathcal{P}_{NW}$ as a function of $\Delta m_{\tilde{g}}$ (top panel) and $\Delta m_{\tilde{t}_1}$ (bottom panel) for $\sqrt{s} = 13$ TeV LHC, and for the benchmark point BP3. The width of the gluino (stop) is taken to be $\Gamma = 5$ GeV.

$pp \to \tilde{g}\tilde{t}_1^* b\bar{\ell}\bar{\nu}$ is given by

$$\begin{aligned}\sigma(pp \to \tilde{g}\tilde{t}_1^* b\bar{\ell}\bar{\nu}) &= \sum_{q_1,q_2} \int dx_1 dx_2 \; f_{q_1/p}(x_1) f_{q_2/p}(x_2) \\ &\times \hat{\sigma}_{\tilde{g}\tilde{g}} \; \mathcal{B}(\tilde{g} \to t\tilde{t}_1^*) \; \mathcal{B}(t \to b\bar{\ell}\bar{\nu}) \qquad (37) \\ &= \sigma_{\tilde{g}\tilde{g}} \; \mathcal{B}(\tilde{g} \to t\tilde{t}_1^*) \; \mathcal{B}(t \to b\bar{\ell}\bar{\nu}).\end{aligned}$$

Equation (36) can also be written in a different form:

$$\mathcal{P}_{NW} = \frac{1}{\sigma_{\tilde{g}\tilde{g}}} \int \frac{d\sigma}{d\bar{\beta}} \mathcal{P}(\bar{\beta}). \qquad (38)$$

The top polarization in the PCM and in the lab frame follow the same formula. The top polarization in lab frame can be derived without referring to the PCM frame by considering the transformation mentioned in Section III (see also Appendix A) [19]. The rotation matrix R of Eq. (28) simply becomes, $R = R_y(-\omega)$. The expression for ω the of the same form as the one the corresponding to Eq. (34) except that $\bar{\beta}$ is replaced by the velocity of the gluino in the lab frame $\beta_{\tilde{g}}^{\rm lab}$. Equation (30) becomes, in this case,

$$\frac{\mathrm{d}\hat{\sigma}}{\mathrm{d}x_\ell \mathrm{d}\cos\theta_{t\ell}} \propto \int \hat{\sigma}_{\tilde{g}\tilde{g}} \Big(1 + \mathcal{P}\cos\omega\cos\theta_{t\ell}\Big) x_\ell(1-x_\ell) \mathrm{d}\Omega_t^{\tilde{g}}. \qquad (39)$$

Following the same steps given in Section III B we get Eq. (38) with $\bar{\beta} \to \beta_{\tilde{g}}^{\rm lab}$.

We now present the numerical validation of our method which is summarized by Eq. (38). We use `MadGraph` [51] to generate events for the processes $pp \to \tilde{g}\tilde{g} \to t\tilde{t}_1^*\tilde{g}$ and $pp \to \tilde{t}_1\tilde{t}_1^* \to t\tilde{\chi}_1^0$, followed by the decay of the top through $t \to b\bar{\ell}\nu$, for the three SUSY benchmark points listed in Table. I. In these simulations, we artificially vary the parameters like width, mass etc. but keep the mixing of stop, and neutralino as constants.

We evaluate the top polarization using different methods for comparisons. Firstly, the top polarization is directly obtained from the MC simulation of the entire decay chain and then using the formula [52]:

$$\mathcal{P}_{MC} = 2\,\frac{N(p_\ell \cdot s_t < 0) - N(p_\ell \cdot s_t > 0)}{N(p_\ell \cdot s_t < 0) + N(p_\ell \cdot s_t > 0)} \qquad (40)$$

where p_ℓ is the momentum of the charged lepton from the top decay and s_t is the longitudinal spin vector satisfying $p_t \cdot s_t = 0$ and $s_t \cdot s_t = -1$. The top spin vector is defined in the frame in which the polarization of the top is defined i.e., the frame of the chosen spin quantization axis of the top.

Secondly, we use the convolution of Eq. (34) or Eq. (35) with the distribution of $\bar{\beta}$ obtained from the same MC simulation to obtain $\mathcal{P}_{NW}$, Eq. (38). Note that the analytical expressions Eq. (34) and (35) assume the validity of NWA and hence use on-shell mass of the other particle. This estimator gives an average of top polarization, weighted by the cross section, over the events of a simulation.

We first set the width of the decaying gluino/stop to $\Gamma = 5$ GeV, justifying NWA. We expect that the result of $\mathcal{P}_{MC}$ and $\mathcal{P}_{NW}$ should agree with each other. This is indeed shown by the top and bottom panels of Fig. 5 which compare these two methods in the gluino and the stop cases, respectively, as a function of $\Delta m_{\tilde{g}}$ or $\Delta m_{\tilde{t}}$. These figures correspond to a pp center of mass energy $\sqrt{s} = 13$ TeV and the benchmark point BP3. The value of rest frame top polarization $\mathcal{P}_0$ is also shown as a function of $\Delta m_{\tilde{g}}$ or $\Delta m_{\tilde{t}}$ for comparison. We can see that $\mathcal{P}_{MC}$ and $\mathcal{P}_{NW}$ converges to $\mathcal{P}_0$ at large values of $\Delta m_{\tilde{g}/\tilde{t}_1}$. This is expected, since the top is highly boosted in the rest frame of the gluino/stop when Δm is large, i.e. $\beta \approx 1$. Any boost of this frame $\bar{\beta}$ which is less than β does not affect the value of top polarization, since $I(\bar{\beta}) \approx 1$ with $\bar{\beta} \ll \beta$, Eq.(32)). This can be understood physically in the following way: in this limit, due to its large mass, gluino is produced with a small velocity $\bar{\beta} \approx 0$. Hence, we expect that the top polarization has to agree with its value in the gluino rest frame. We do not show the corresponding figures for the other two benchmark points as they do show the same good agreement between $\mathcal{P}_{MC}$ and $\mathcal{P}_{NW}$ and convergence to $\mathcal{P}_0$ at large values of $\Delta m_{\tilde{g}}$ or $\Delta m_{\tilde{t}}$.

As an illustration of the case where the decaying gluino/stop has a finite width, we show in Fig. 6 (Fig. 7) the comparison of values of top polarization obtained through $\mathcal{P}_{MC}$ and $\mathcal{P}_{NW}$ for the case where the gluino (stop) has a width $\Gamma = 200$ GeV. In each figure, we present results for two pp center of mass energies $\sqrt{s} = 7$ TeV and $\sqrt{s} = 13$ TeV and for a benchmark point BP1.

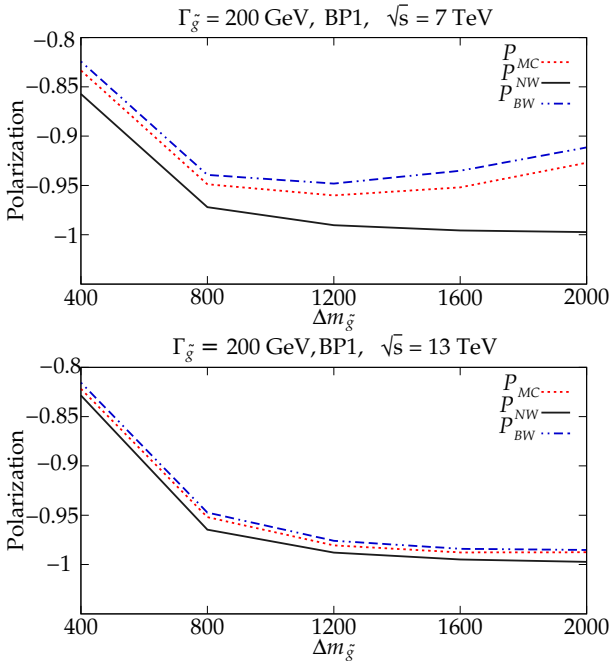

FIG. 6. Comparison of top polarization, in the case of gluino decay, evaluated in the three methods: $\mathcal{P}_{MC}$, $\mathcal{P}_{NW}$ and $\mathcal{P}_{BW}$, for $\sqrt{s} = 7$ TeV(top) and $\sqrt{s} = 13$ TeV(bottom), as a function of $\Delta m_{\tilde{g}}$. The width of the gluino is taken to be $\Gamma = 200$ GeV. The parameters other than $m_{\tilde{g}}, \Gamma_{\tilde{g}}$ correspond to the benchmark point BP1.

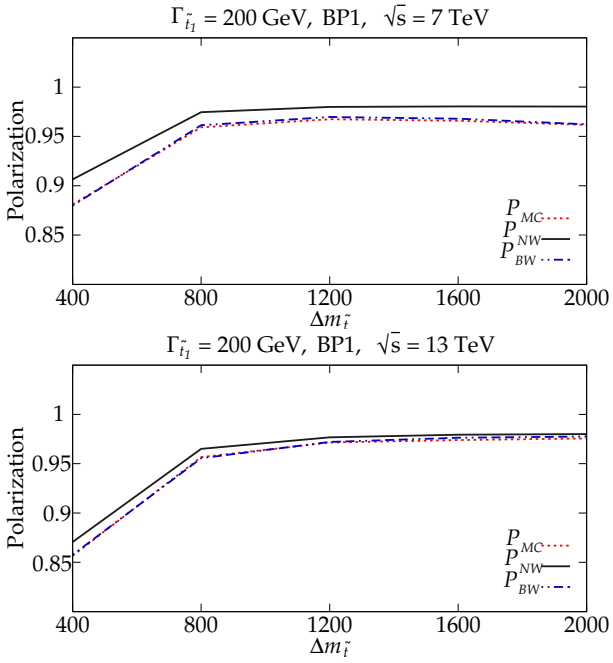

FIG. 7. Comparison of top polarization, in the case of stop decay, evaluated in the three methods: $\mathcal{P}_{MC}$, $\mathcal{P}_{NW}$ and $\mathcal{P}_{BW}$, for $\sqrt{s} = 7$ TeV(top) and $\sqrt{s} = 13$ TeV(bottom), as a function of $\Delta m_{\tilde{t}_1}$. The width of the stop and the other parameters are the same as those of Fig. 6.

For the range of gluino/stop masses which are considered here, the mother particle (gluino/stop) is mostly off-shell when $\sqrt{s} = 7$ TeV and mostly on-shell for $\sqrt{s} = 13$ TeV. Hence, we expect that the results of $\mathcal{P}_{NW}$ may show deviation with those of $\mathcal{P}_{MC}$ for the case $\sqrt{s} = 7$ TeV, and expect better agreement between the two methods for $\sqrt{s} = 13$ TeV. The figures Fig. 6 and Fig. 7 show that this is indeed the case. We emphasize here that our method $\mathcal{P}_{NW}$ is only an approximation which should work when the NWA for the mother particle is applicable. However, we can modify $\mathcal{P}_{NW}$ to include, at least partly, the effects which arise from finite width of the mother particle through a procedure which is explained in the following section.

V. INCLUSION OF FINITE WIDTH EFFECTS

The validity of narrow-width-approximation, with reference to BSM physics, has been a subject of careful investigation [53–55]. We, on the other hand, take a simple minded approach to address the presence of large widths for the mother particles and test the validity of our modified estimator, $\mathcal{P}_{BW}$.

This estimator is obtained when the mass of the mother particle is taken to be $M_{\tilde{g}}^2 = p_{\tilde{g}}^2 (M_{\tilde{t}_1}^2 = p_{\tilde{t}_1}^2)$, where $p_{\tilde{g}}$ ($p_{\tilde{t}_1}$) is the momentum of the mother, in place of it's on-shell mass $m_{\tilde{g}} (m_{\tilde{t}_1})$. In addition to this, the invariant mass is assumed to be distributed as a Breit-Wigner-like distribution. In other words, the top polarization is obtained by introducing an additional convolution over the mass of the decaying heavy particle:

$$\mathcal{P}_{BW} = \frac{1}{\sigma_{XX}} \int_{M_{\rm min}^2}^{M_{\rm max}^2} dM^2 \Delta_{BW}(M,m) \times \int f_{q_1/p}(x_1) f_{q_2/p}(x_2) \hat{\sigma}_{XX,M}(\hat{s}) \mathcal{P}(\bar{\beta}_M) \tag{41}$$

where $\hat{\sigma}_{XX,M}$ (XX=$\tilde{g}\tilde{g}$ or $\tilde{t}_1\tilde{t}_1$) and $\bar{\beta}_M$ are evaluated for a gluino or a stop mass of M: $\bar{\beta}_M = \sqrt{1 - 4M^2/\hat{s}}$.

$$\sigma_{XX} = \int_{M_{\rm min}^2}^{M_{\rm max}^2} dM^2 \Delta_{BW}(M,m) \times \int f_{q_1/p}(x_1) f_{q_2/p}(x_2) \hat{\sigma}_{XX,M}(\hat{s}) \tag{42}$$

The Breit-Wigner factor $\Delta_{BW}(M,m)$ is given by

$$\Delta_{BW}(M,m) = \frac{1}{(M^2 - m^2)^2 + M^2\Gamma^2}. \tag{43}$$

The limits of the integration viz., $M_{\rm min}$ and $M_{\rm max}$ can be thought of as the minimum and the maximum mass of the off-shell gluino and are specified usually in the form of an integer (n) that represents the 'distances' of $M_{\rm max,min}$ from the on-shell mass in units of the width: $M_{\rm min,max} = m_{\tilde{g}} \pm n\Gamma_{\tilde{g}}$. The equation given above, Eq. (41) can also

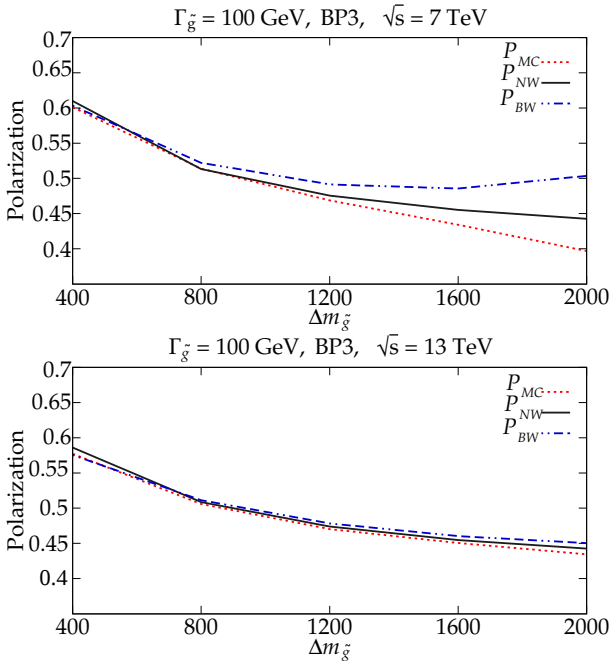

FIG. 8. Comparison of top polarization evaluated in the three methods: $\mathcal{P}_{MC}$, $\mathcal{P}_{NW}$ and $\mathcal{P}_{BW}$, as a function of $\Delta m_{\tilde{g}}$, for two pp center of mass energies $\sqrt{s} = 7$ TeV(top), $\sqrt{s} = 13$ TeV(bottom), in the case of gluino decay. The width of the gluino is taken to be $\Gamma = 100$ GeV. The parameters other than $m_{\tilde{g}}, \Gamma_{\tilde{g}}$ correspond to the benchmark point BP3.

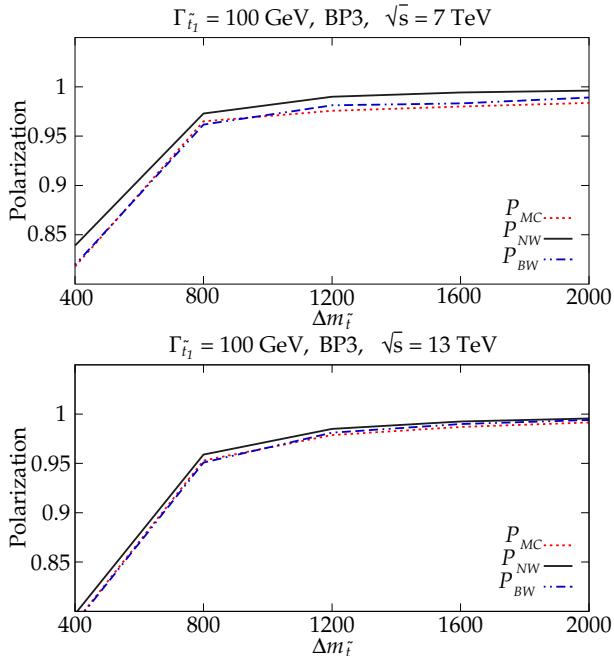

FIG. 9. Comparison of top polarization evaluated in the three methods: $\mathcal{P}_{MC}$, $\mathcal{P}_{NW}$ and $\mathcal{P}_{BW}$, as a function of $\Delta m_{\tilde{t}}$, for two pp center of mass energies $\sqrt{s} = 7$ TeV (top), $\sqrt{s} = 13$ TeV(bottom), in the case of stop decay. The width of the stop and the other parameters are the same as those in Fig. 8.

be written as

$$\mathcal{P}_{BW} = \frac{1}{\sigma_{XX}} \int_{M^2_{\rm min}}^{M^2_{\rm max}} dM^2 \Delta_{BW}(M, m) \times \int \frac{d\sigma_{XX}}{d\beta_M} \mathcal{P}(\beta_M) d\beta_M. \quad (44)$$

We note that this procedure is, at best, only an approximate one. In the case of gluino, there are additional spin correlation between the production and decay of a gluino pair, when the gluino is off-shell [56–58]. Equation (19), based on which the expressions Eq. (34) and Eq. (35) have been derived, should be modified to include the off-shell effects:

$$\sum_\lambda u(p)\bar{u}(p) = \not{p} + m + \frac{\not{l}}{2p \cdot l}(m^2 - p^2), \quad (45)$$

where l is a light-like four-vector and m is the physical on-shell mass [58]. In the case of stop decay, we naively expect that the inclusion of Breit-Wigner distribution for the mass of the stop as given in Eq. (44) should be sufficient, as the stop is a scalar. However, as we discuss below, even in the case of stop decay, the top polarization calculated using Eq. (44) can deviate from the actual value, at large values of $\Delta m_{\tilde{t}}$. In the previous section, we have described the polarization $\mathcal{P}_{MC}$ and $\mathcal{P}_{NW}$, as given in Fig. 6 and 7, which correspond to cases where the mother particle has a finite width. These figures also show the polarization $\mathcal{P}_{BW}$, Eq. (44). In the top panels of Fig. 6 and 7 which correspond to the case $\sqrt{s} = 7$ TeV, one can clearly see the improvement one obtains in $\mathcal{P}_{BW}$ over the that of $\mathcal{P}_{NW}$. Although $\mathcal{P}_{BW}$ differs from $\mathcal{P}_{MC}$ particularly for large values of $\Delta m_{\tilde{g}}$ (or $\Delta m_{\tilde{t}}$) the difference is much smaller compared to the difference between $\mathcal{P}_{MC}$ and $\mathcal{P}_{NW}$. When the pp center of mass energy $\sqrt{s}$ is increased to 13 TeV, as shown on the bottom panels of Figs 6 and 7, the three methods agree with each other within a few percent. As mentioned before, this is due to the increase in the relative contribution of on-shell gluino/stop at $\sqrt{s} = 13$ TeV. The deviations between the $\mathcal{P}_{BW}$ and $\mathcal{P}_{MC}$ also depend upon the benchmark point chosen. In Fig. 8 and Fig. 9 we have shown the comparisons of the three methods for the benchmark point BP3. In this case, the inclusion of an additional convolution over a Breit-Wigner distribution of mother particle mass, as in $\mathcal{P}_{BW}$ does not improve the results of $\mathcal{P}_{NW}$, for $\sqrt{s} = 7$ TeV. In fact, the difference between $\mathcal{P}_{BW}$ and $\mathcal{P}_{MC}$ is greater than that between $\mathcal{P}_{NW}$ and $\mathcal{P}_{MC}$. On the other hand, for $\sqrt{s} = 13$ TeV, all the three method agree, as they do in the previous cases. Hence, we see that an inclusion of a convolution of Breit-Wigner distribution for the mother particle mass alone does not always lead to the actual value of top polarization. We believe that the neglect of additional spin-correlations in the case of gluino, as mentioned before, could be a source of this discrepancy. This could also be the possible reason for the discrepancy between $\mathcal{P}_{BW}$ and $\mathcal{P}_{MC}$ being

particularly large for the case of gluino decay compared to the case of stop decay. In view of the fact that for $\sqrt{s} = 13$ TeV, all the three results agree, we propose that we can stick to $\mathcal{P}_{NW}$ rather than use $\mathcal{P}_{BW}$. In any case, our method $\mathcal{P}_{NW}$ is valid only when the contribution of on-shell gluino/stop pairs to the cross section dominates over the corresponding contribution from the off-shell pairs. In these cases, we have already established that $\mathcal{P}_{NW}$ gives a reasonable approximation to the actual Monte Carlo value of top polarization. The advantage of $\mathcal{P}_{NW}$, though only an approximation, is that it allows for a fast estimation of the top polarization, in any frame, when the velocity distribution of the produced mother particle alone is available. Detailed simulation of the decay of the mother particle is then not necessary.

VI. SUMMARY

In this work, we propose a simple estimator to measure the polarization of the top produced in the decays of heavy particles, in any frame, given its value in the rest frame of the decaying particle. We quantify the kinematical factors that relate the top polarization in the two frames. We find that the top polarization in the lab frame depends only on the magnitude of the velocity and not on the angles of emission of the mother particle in the lab frame. The polarization estimators $\mathcal{P}_{NW}$ and $\mathcal{P}_{BW}$, in the lab frame, are obtained by convoluting the expression for top polarization with the velocity distribution of the mother particle in the lab frame.

The estimator $\mathcal{P}_{NW}$ assumes mother particle to be on-shell and yields values very close to the true one, $\mathcal{P}_{MC}$, when the mother particle has narrow width. For a wider mother particle, we use $\mathcal{P}_{BW}$ which includes the finite-width effects by a convolution with Breit-Wigner distribution of the mass of the mother particle. $\mathcal{P}_{BW}$ works better than $\mathcal{P}_{NW}$ for stop with large width. For a wide gluino also $\mathcal{P}_{BW}$ works better than $\mathcal{P}_{NW}$ when majority of the events corresponds to the on-shell gluino. In the case of a heavy and wide gluino, which is pre-dominantly produced off-shell, both $\mathcal{P}_{NW}$ and $\mathcal{P}_{BW}$ can deviate from $\mathcal{P}_{MC}$ by an amount as large as 0.05 for specific mixing angles. However, when the mother particle is dominantly produced on-shell, as in the case of high *pp* center of mass energy, these estimators can be used to obtain a fast and accurate estimation of the top polarization in the lab frame. In the case of gluino decay, we point out that the polarization of the produced top can be used as a direct probe of mixing angle in the stop sector, in the scenario of a 'natural supersymmetry'.

ACKNOWLEDGMENTS

One of the authors (APV) would like to thank Gaurav Mendiratta for his constant encouragements and discussions throughout the duration of the project. He also thanks Rafiqul Rahman for his kind help and IISER, Kolkata for hospitality, during his stay as a visitor. We also thank Saurabh D. Rindani for taking part in the early stages of this project.

Appendix A: Rotation of helicity states under Lorentz boosts

In this appendix, we derive the expressions for the helicity rotation angles ω, χ that are mentioned in the text. We denote the operators corresponding to rotations and Lorentz transformations by R and L. The same symbols denote the corresponding operations themselves. We denote the helicity states by $|p, \lambda\rangle$. Under a Lorentz transformation L, the helicity states transform as $|p, \lambda\rangle \to L|p, \lambda\rangle = |p', \rangle$, with $p' = L\ p$. The state $|p', \rangle$ is a state with definite momentum in the Lorentz transformed frame. It does not have a definte helicity in this frame. Thee reason is that the helicity is not conserved under a general Lorentz transformation. However, it is conserved as long as the Lorentz transformation is along the direction of motion of the particle. It is also invariant under rotations. With this information, we try to obtain an expression for $|p', \rangle$ in terms of the helicity states $|p', \lambda'\rangle$ of the new frame. We focus only on the case of a massive particle.

Consider a helicity state $|p, \lambda\rangle$ of a particle with momentum $p = (p^0, |\vec{p}| \sin\theta\cos\phi, |\vec{p}| \sin\theta \sin\phi, |\vec{p}| \cos\theta)$ and helicity λ, in a given frame. The following sequence of transformation map the helicity state into a state $|m, s_z = \lambda\rangle$ in the rest frame of the particle:

$$L_z^{-1}(\beta = |\vec{p}|/p^0) R_y^{-1}(\theta) R_z^{-1}(\phi) |p, \lambda\rangle = |m, s_z = \lambda\rangle \tag{A1}$$

where s_z denotes the eigenvalue of the z-component of spin operator $\vec{S}$. The sequence of two rotations $R_y^{-1}(\theta) R_z^{-1}(\phi)$ bring the direction of momentum of the particle to the z-axis and the Lorentz transformation L_z^{-1} takes the resulting state $||\vec{p}|\hat{z}, \lambda\rangle$ to a state in the rest frame of the particle which we take as the eigenstate of S_z operator. We can also invert this equation and write helicity state of the particle in terms of $|m, s_z = \lambda\rangle$:

$$|p, \lambda\rangle R_z(\phi) R_y(\theta) L_z(\beta = |\vec{p}|/p^0) |m, s_z = \lambda\rangle. \tag{A2}$$

We regard this expression as the *definition* of the helicity state of the particle. For convenience we define the sequence of operations on the right hand side of the above expression as an operation $h(p)$:

$$h(p) \equiv R_z(\phi) R_y(\theta) L_z(\beta = |\vec{p}|/p^0). \tag{A3}$$

We now turn to the case of the top quark produced in the decay of a gluino. The parton center of mass (PCM) frame, as mentioned before, can be reached from the top rest frame (t rest) with the following transformations:

$$t\text{ - rest} \xrightarrow{h(p_t^{\rm PCM})} \text{PCM} \tag{A4}$$

where $p_t^{\rm PCM}$ denotes the momentum of the top in the PCM frame. This transformation maps the states $|m, s_z = \lambda\rangle$ in the top rest frame to the top helicity states in the PCM frame. There is no change in the helicity of the top quark, in this transformation.

$$|p_t^{\rm PCM}, \lambda\rangle = h(p_t^{\rm PCM})|m, s_z = \lambda\rangle. \tag{A5}$$

Now the same PCM frame can also be reached from the top rest frame through the following sequence of transformations:

$$t\text{-rest} \xrightarrow{h(p_t^{\tilde g})} \tilde g\text{-rest} \xrightarrow{h(p_{\tilde g}^{\rm PCM})} \text{PCM}. \tag{A6}$$

where $p_t^{\tilde g}$ and $p_{\tilde g}^{\rm PCM}$ denote the momenta of the top in the gluino rest frame and the momentum of the gluino in the PCM frame respectively. We denote the velocity and the angles of the gluino in the PCM frame by $\bar\beta$, $\theta_{\tilde g}$ and $\phi_{\tilde g}$ as in the main text. The above expression means that we first go to the gluino rest frame through the helicity preserving transformation $h(p_t^{\tilde g})$ and reach the PCM frame by $h(p_{\tilde g}^{\rm PCM}) \equiv R_z(\phi_{\tilde g})R_y(\theta_{\tilde g})L_z(\bar\beta)$. Note that in the transformation from the gluino rest frame to the PCM frame, the Lorentz transformation $L_z(\bar\beta)$ acts along the z-direction while the top with $p_t^{\tilde g}$ is moving at an angle θ to the z-axis. This Lorentz transformation does not preserve the helicity of the top. The following transformations are just rotations which do not further affect the helicity state of the top. As a result, the helicity state of the top obtained through the transformations of Eq. (A5) and those obtained through Eq. (A6) are different. Now,

$$h(p_{\tilde g}^{\rm PCM})h(p_t^{\tilde g})|m, s_z = \lambda\rangle = |p_t^{\rm PCM}, \rangle \tag{A7}$$

as in Eq. (A1). Inserting $h(p_t^{\rm PCM})h^{-1}(p_t^{\rm PCM}) = 1$ in Eq. (A7), we get,

$$h(p_t^{\rm PCM})\left[h^{-1}(p_t^{\rm PCM})h(p_{\tilde g}^{\rm PCM})h(p_t^{\tilde g})\right]|m, s_z = \lambda\rangle = |p_t^{\rm PCM}, \rangle. \tag{A8}$$

Now, we can easily see that the terms in $[\cdots]$ correspond to a rotation (R) in the rest frame of the top quark, since these set of transformations map $p_t^t = (m, \vec 0)$ to itself: $h(p_t^{\tilde g})p_t^t = p_t^{\tilde g}$, $h(p_{\tilde g}^{\rm PCM})p_t^{\tilde g} = p_t^{\rm PCM}$ and $h^{-1}(p_t^{\rm PCM})p_t^{\rm PCM} = p_t^t = (m, \vec 0)$. Since,

$$R|m, s_z = \lambda\rangle = R_{\lambda,\lambda'}|m, s_z = \lambda'\rangle \tag{A9}$$

with $R_{\lambda,\lambda'}$ being the elements of this rotation matrix, we get, from Eq. (A8),

$$|p_t^{\rm PCM}, \rangle = h(p_t^{\rm PCM})R_{\lambda,\lambda'}|m, s_z = \lambda'\rangle = |p_t^{\rm PCM}, \lambda'\rangle. \tag{A10}$$

Hence, the effect of the sequence of transformations $h(p_{\tilde g}^{\rm PCM})$ on the helicity states of top $|p_t^{\tilde g}, \lambda\rangle$ is equivalent to a rotation in the helicity states of the top in the *transformed* frame. The rotation R is given by the following expression:

$$R = h^{-1}(p_t^{\rm PCM})h(p_{\tilde g}^{\rm PCM})h(p_t^{\tilde g}) \tag{A11}$$

This expression is difficult to evaluate. We can break down this rotation into a product of two rotations by inserting $h(p_t')h^{-1}(p_t') = 1$ where p_t' is momentum of the top in an intermediate step in the transformation from gluino rest frame to the PCM frame: $p_t' = L_z(\bar\beta)p_t^{\tilde g}$. Note that $p_t^{\rm PCM} = h(p_{\tilde g}^{\rm PCM})p_t^{\tilde g} = R_z(\phi_{\tilde g})R_y(\theta_{\tilde g})L_z(\bar\beta)p_t^{\tilde g} = R_z(\phi_{\tilde g})R_y(\theta_{\tilde g})p_t'$. With this, the expression for R becomes,

$$R = \left[h^{-1}(p_t^{\rm PCM})h(p_t')\right]\left[h^{-1}(p_t')h(p_{\tilde g}^{\rm PCM})h(p_t^{\tilde g})\right]. \tag{A12}$$

By a direct computation, we can establish that the two terms correspond to rotations about the z-axis and y-axis in the top rest frame, respectively, through angles χ and ω. $R = R_z(\chi)R_y(\omega)$. The expressions for χ and ω are given below. In these expressions, Eq. (A13) and Eq. (A14), $p_t^{\tilde g}$ is given in terms of its velocity β, and the angles θ and ϕ in the gluino rest frame (the subscripts and the superscripts have been dropped) and the angles of $p_t^{\rm PCM}$ by θ'' and ϕ''. The gluino momentum $p_{\tilde g}^{\rm PCM}$ is given in terms of its velocity $\bar\beta$ and the angles $\bar\theta$ and $\bar\phi$ in the PCM frame (the subscript and the superscript have been dropped).

$$\cos\omega = \frac{(\beta + \bar\beta\cos\theta)}{\sqrt{\beta^2 + \bar\beta^2 - \beta^2\bar\beta^2\sin^2\theta + 2\beta\bar\beta\cos\theta}}, \tag{A13}$$
$$\sin\omega = \frac{\bar\beta\sin\theta}{\gamma\sqrt{\beta^2 + \bar\beta^2 - \beta^2\bar\beta^2\sin^2\theta + 2\beta\bar\beta\cos\theta}},$$

and

$$\cos\chi = \cos\phi\cos\Delta\phi - \sin\Delta\phi\cos\bar\theta\sin\phi, \tag{A14}$$
$$\sin\chi = -\frac{\sin\Delta\phi\sin\bar\theta\sqrt{\bar\beta^2 + \beta^2 - \bar\beta^2\beta^2\sin^2\theta + 2\bar\beta\beta\cos\theta}}{\sqrt{1-\bar\beta^2}\beta\sin\theta},$$

where $\Delta\phi = \bar\phi - \phi''$.

The lab frame can be reached from the top rest frame by following two transformations:

$$t\text{-rest} \xrightarrow{h(p_t^{\tilde g})} \tilde g\text{-rest} \xrightarrow{h(p_{\tilde g}^l)\equiv R_z(\phi_{\tilde g}^l)R_y(\theta_{\tilde g}^l)L_z(\beta_{\tilde g}^l)} \text{lab} \tag{A15}$$

and the helicity preserving one,

$$t\text{-rest} \xrightarrow{h(p_t^l)\equiv R_z(\phi_t^l)R_y(\theta_t^l)L_z(\beta_t^l)} \text{lab}. \tag{A16}$$

In these expressions, the quantities which are defined in the lab frame are denoted by a superscript l. The helicity states of the top obtained from $|m, s_z = \lambda\rangle$ in the rest frame of the top through the transformation of Eq. (A15) is different from those obtained through the transformation of Eq. (A16). Using $h^{-1}(p_t^l)h(p_t^l) = 1$ and following the same steps as in the previous case, we obtain

$$h(p_{\tilde g}^l)h(p_t^{\tilde g})|m, s_z = \lambda\rangle = |p_t^l, \rangle = R_{\lambda,\lambda'}|p_t^l, \lambda'\rangle \tag{A17}$$

with $R = h^{-1}(p_t^l)h(p_{\tilde g}^l)h(p_t^{\tilde g})$. This is of the same form as $R_y = h^{-1}(p_t')h(p_{\tilde g}^{\rm PCM})h(p_t^{\tilde g})$ of Eq. (A12). Hence, the expressions for the rotation angle ω , in this case, can be obtained from Eq. (A13) through the replacement: $\bar\beta \to \bar\beta^l$.

[1] M. Beneke et al., in *1999 CERN Workshop on standard model physics (and more) at the LHC, CERN, Geneva, Switzerland, 25-26 May: Proceedings* (2000), hep-ph/0003033, URL `http://weblib.cern.ch/abstract?CERN-TH-2000-100`.

[2] T. Han, Int. J. Mod. Phys. **A23**, 4107 (2008), 0804.3178.

[3] W. Bernreuther, J. Phys. **G35**, 083001 (2008), 0805.1333.

[4] F.-P. Schilling, Int. J. Mod. Phys. **A27**, 1230016 (2012), 1206.4484.

[5] E. Barberis, Int. J. Mod. Phys. **A28**, 1330027 (2013).

[6] S. Jabeen, Int. J. Mod. Phys. **A28**, 1330038 (2013).

[7] C. T. Hill and E. H. Simmons, Phys. Rept. **381**, 235 (2003), [Erratum: Phys. Rept.390,553(2004)], hep-ph/0203079.

[8] M. Schmaltz and D. Tucker-Smith, Ann. Rev. Nucl. Part. Sci. **55**, 229 (2005), hep-ph/0502182.

[9] M. Jezabek and J. H. Kuhn, Nucl.Phys. **B320**, 20 (1989).

[10] A. Czarnecki, M. Jezabek, and J. H. Kuhn, Nucl.Phys. **B351**, 70 (1991).

[11] G. L. Kane, G. A. Ladinsky, and C. P. Yuan, Phys. Rev. **D45**, 124 (1992).

[12] W. Bernreuther, D. Heisler, and Z.-G. Si, JHEP **12**, 026 (2015), 1508.05271.

[13] R. Schwienhorst, C. P. Yuan, C. Mueller, and Q.-H. Cao, Phys. Rev. **D83**, 034019 (2011), 1012.5132.

[14] G. Mahlon and S. J. Parke, Phys. Lett. **B476**, 323 (2000), hep-ph/9912458.

[15] M. Perelstein and A. Weiler, JHEP **03**, 141 (2009), 0811.1024.

[16] I. Low, Phys. Rev. **D88**, 095018 (2013), 1304.0491.

[17] G. Belanger, R. M. Godbole, S. Kraml, and S. Kulkarni (2013), 1304.2987.

[18] G. Belanger, R. M. Godbole, L. Hartgring, and I. Niessen, JHEP **05**, 167 (2013), 1212.3526.

[19] J. Shelton, Phys. Rev. **D79**, 014032 (2009), 0811.0569.

[20] K.-i. Hikasa, J. M. Yang, and B.-L. Young, Phys. Rev. **D60**, 114041 (1999), hep-ph/9908231.

[21] M. Arai, K. Huitu, S. K. Rai, and K. Rao, JHEP **08**, 082 (2010), 1003.4708.

[22] K. Agashe, A. Belyaev, T. Krupovnickas, G. Perez, and J. Virzi, Phys. Rev. **D77**, 015003 (2008), hep-ph/0612015.

[23] D. Choudhury, R. M. Godbole, R. K. Singh, and K. Wagh, Phys. Lett. **B657**, 69 (2007), 0705.1499.

[24] R. M. Godbole, K. Rao, S. D. Rindani, and R. K. Singh, JHEP **11**, 144 (2010), 1010.1458.

[25] S. Gopalakrishna, T. Han, I. Lewis, Z.-g. Si, and Y.-F. Zhou, Phys. Rev. **D82**, 115020 (2010), 1008.3508.

[26] K. Huitu, S. Kumar Rai, K. Rao, S. D. Rindani, and P. Sharma, JHEP **04**, 026 (2011), 1012.0527.

[27] S. D. Rindani and P. Sharma, JHEP **11**, 082 (2011), 1107.2597.

[28] S. S. Biswal, S. D. Rindani, and P. Sharma, Phys. Rev. **D88**, 074018 (2013), 1211.4075.

[29] J. A. Aguilar-Saavedra and S. A. dos Santos, Phys. Rev. **D89**, 114009 (2014), 1404.1585.

[30] J. Cao, L. Wu, and J. M. Yang, Phys. Rev. **D83**, 034024 (2011), 1011.5564.

[31] D. Choudhury, R. M. Godbole, S. D. Rindani, and P. Saha, Phys. Rev. **D84**, 014023 (2011), 1012.4750.

[32] D. Krohn, T. Liu, J. Shelton, and L.-T. Wang, Phys. Rev. **D84**, 074034 (2011), 1105.3743.

[33] A. Falkowski, G. Perez, and M. Schmaltz, Phys. Rev. **D87**, 034041 (2013), 1110.3796.

[34] R. M. Godbole, L. Hartgring, I. Niessen, and C. D. White, JHEP **01**, 011 (2012), 1111.0759.

[35] M. Baumgart and B. Tweedie, JHEP **08**, 072 (2013), 1303.1200.

[36] J. Cao, K. Hikasa, L. Wang, L. Wu, and J. M. Yang, Phys. Rev. **D85**, 014025 (2012), 1109.6543.

[37] S. Fajfer, J. F. Kamenik, and B. Melic, JHEP **08**, 114 (2012), 1205.0264.

[38] S. Chatrchyan et al. (CMS), Phys. Lett. **B716**, 30 (2012), 1207.7235.

[39] G. Aad et al. (ATLAS), Phys. Lett. **B716**, 1 (2012), 1207.7214.

[40] L. J. Hall, D. Pinner, and J. T. Ruderman, JHEP **04**, 131 (2012), 1112.2703.

[41] A. Arbey, M. Battaglia, A. Djouadi, F. Mahmoudi, and J. Quevillon, Phys. Lett. **B708**, 162 (2012), 1112.3028.

[42] H. Baer, V. Barger, P. Huang, and X. Tata, JHEP **05**, 109 (2012), 1203.5539.

[43] V. Barger, P. Huang, M. Ishida, and W.-Y. Keung, Phys. Lett. **B718**, 1024 (2013), 1206.1777.

[44] M. W. Cahill-Rowley, J. L. Hewett, A. Ismail, and T. G. Rizzo, Phys. Rev. **D86**, 075015 (2012), 1206.5800.

[45] M. Drees and J. S. Kim (2015), 1511.04461.

[46] M. M. Nojiri, Phys. Rev. **D51**, 6281 (1995), hep-ph/9412374.

[47] R. Kitano, T. Moroi, and S.-f. Su, JHEP **12**, 011 (2002), hep-ph/0208149.

[48] E. Boos, H. U. Martyn, G. A. Moortgat-Pick, M. Sachwitz, A. Sherstnev, and P. M. Zerwas, Eur. Phys. J. **C30**, 395 (2003), hep-ph/0303110.

[49] T. Gajdosik, R. M. Godbole, and S. Kraml, JHEP **09**, 051 (2004), hep-ph/0405167.

[50] C. Bourrely, J. Soffer, and E. Leader, Phys. Rept. **59**, 95 (1980).

[51] J. Alwall, R. Frederix, S. Frixione, V. Hirschi, F. Maltoni, O. Mattelaer, H. S. Shao, T. Stelzer, P. Torrielli, and M. Zaro, JHEP **07**, 079 (2014), 1405.0301.

[52] F. Boudjema and R. K. Singh, JHEP **07**, 028 (2009), 0903.4705.

[53] D. Berdine, N. Kauer, and D. Rainwater, Phys. Rev. Lett. **99**, 111601 (2007), hep-ph/0703058.

[54] C. F. Uhlemann and N. Kauer, Nucl. Phys. **B814**, 195 (2009), 0807.4112.

[55] N. Kauer, Phys. Lett. **B649**, 413 (2007), hep-ph/0703077.

[56] R. Vega and J. Wudka, Phys. Rev. **D53**, 5286 (1996), [Erratum: Phys. Rev.D56,6037(1997)], hep-ph/9511318.

[57] A. Ballestrero and E. Maina, Phys. Lett. **B350**, 225 (1995), hep-ph/9403244.

[58] P. Richardson, JHEP **11**, 029 (2001), hep-ph/0110108.